Geotech Geol Eng (2018) 36:3731–3741
https://doi.org/10.1007/s10706-018-0567-y

ORIGINAL PAPER

# Non-linear Shear Strength Criterion for a Rock Joint with Consideration of Friction Variation

**Hu Wang · Hang Lin**

Received: 2 February 2018 / Accepted: 3 May 2018 / Published online: 9 May 2018


**Abstract** Under shearing, joint asperities get sheared off and damaged. Moreover, shearing and sliding and the interaction between normal and shear stresses occur simultaneously. The nonlinearity of the shear strength envelope is closely related to the joint material, normal stress level, and morphological characteristics. This study analyzed the correlation of the friction angle with the normal stress level to overcome overestimation or underestimation at relatively low or high normal stress levels in the JRC–JCS empirical model. A hyperbolic function was adopted to describe the degradation of friction for different normal stress levels, and the modified non-linear shear criterion $\tau = \sigma_n \tan(\phi_r + \Delta\phi/(1 + a\sigma_n/\mathrm{JCS}))$ was proposed. Furthermore, the proposed model avoids direct connection to the surface morphology, which is convenient for practical use. Statistical analysis of the experimental data and comparison with the JRC–JCS model verified the validity of the proposed model and present an excellent method for characterizing the non-linearity of the failure envelope for the rock joint.

**Keywords** Rock joint · Direct shear test · Shear strength criterion · Nonlinearity · Peak friction angle

H. Wang · H. Lin (✉)
School of Resources and Safety Engineering, Central South University, Changsha 410083, Hunan, China
e-mail: whwhclyy@163.com

H. Lin
e-mail: linhangabc@126.com

**List of symbols**

| | |
|---|---|
| $\sigma_n$ | Normal stress |
| $\phi$ | Friction angle |
| $\sigma_t$ | Tensile strength |
| $\sigma_T$ | Transition stress in Patton model |
| $\phi_P$ | Friction angle of peak shear strength |
| $\phi_b$ | Basic friction angle |
| $d_n$ | Peak dilation angle |
| $s_n$ | Contribution of asperities degradation in friction angle |
| $\phi_r$ | Residual friction angle |
| $\tau$ | Peak shear strength |
| JRC | Joint roughness coefficient |
| JCS | Joint compressive strength |
| $P_N$ | Median angle pressure in Maksimović model |
| $c_T$ | Apparent cohesion in Maksimović model |
| $\phi_{MAX}$ | Friction angle of the initial surface roughness of the discontinuity |
| $\sigma_c$ | Uniaxial compressive of intact rock |
| $\Delta\phi$ | Difference between $\phi_{MAX}$ and $\phi_r$ |

## 1 Introduction

Discontinuities make a rock mass a discontinuous system because of its relatively poor mechanical properties with respect to rocks. Rock joints considerably influence the instability of rock masses (Serrano et al. 2014; Tang and Wong 2016). Hence, the

shear mechanical behavior of joints has long attracted the interest of many researchers (Asadollahi and Tonon 2010; Wan et al. 2018). Numerous shear strength criteria, including empirical (Tang and Wong 2016; Yang et al. 2016; Tang et al. 2016; Xia et al. 2014; Grasselli 2006) and theoretical approaches (Misra 2002; Homand et al. 2001), have been reported in the literature. Patton (1966) proposed a bilinear shear strength criterion based on an experiment on a regular saw-tooth triangular asperity designed to capture two key mechanisms of asperity, namely, sliding and shearing (Bahaaddini et al. 2013). In this model, the failure envelope consists of two linear segments that intersect at the normal stress $\sigma_T$ known as the transition stress. For normal stresses, in which $\sigma_n$ is less than $\sigma_T$, the rock sliding along the joint asperities and the shear strength are governed by frictional resistance. The shear strength above the transition stress is governed by the shearing of asperities with cohesion of joint wall materials and residual friction angle. Based on extensive experiments on natural rock joints, Barton and Choubey (1977) proposed an empirical law (the JRC–JCS criterion) of friction for rock joints that can be used to extrapolate and predict shear strength data in which the shear strength originates from frictional resistance only. This model is the most widely accepted in practice (Maksimović 1996).

Quantification of surface morphology was introduced into the shear strength criteria (Tang and Wong 2016; Tang et al. 2016; Grasselli 2006; Homand et al. 2001; Zhang et al. 2016) to better understand the nonlinearity of the failure envelope because of the continuous study of surface morphology. However, the description of surface morphology evolution, which is impractical in practice, requires topographical measurements prior to and after each shear test. Thus, the shear strength criteria that use surface morphology characteristics included certain limitations in shear strength prediction. Many studies (Grasselli and Egger 2003) have also shown that friction is correlated with the rock joint material, normal stress level, and surface morphology. Thereafter, researchers (Yang et al. 2016; Tang et al. 2016; Grasselli 2006; Zhang et al. 2016) established more complicated shear strength criteria to overcome the subjective determination of the joint roughness coefficient (JRC), and the coefficient always represents the influence of the surface morphology on friction in these models.

The nonlinearity of the shear strength envelope is closely related to the joint material, normal stress level, and morphology characteristics. Under shearing, joint asperities get sheared off and damaged, and the shearing and sliding as well as the interaction between normal and shear stresses occur simultaneously. In this study, the non-linear variation of the peak friction angle was studied in terms of the nonlinear failure envelope, and a hyperbolic function was proposed to describe the non-linear shear strength criterion for rock joints. A statistical analysis of the experimental data and a comparison with the JRC–JCS model were conducted to verify the validity of the model.

## 2 Non-linear Failure Envelope and Friction Angle Variation

Shearing and sliding simultaneously occur (Bahaaddini et al. 2013) for real rock joints under shearing. At the same time, the course of shearing is governed by normal stress, which restrains the dilatancy effect and affects the joint surface contact. Bandis et al. (1983) used the terms matched and mismatched joints as interlocked and dislocated joints for a natural joint, respectively. Zhao (1997) applied the joint matching coefficient (JMC) to develop the JRC–JMC shear criteria. Shear-off and damage of joint asperities exists in either matched or mismatched joints, and thus, the failure envelope is non-linear (Barton 2013). Homand et al. (2001) studied the shearing of an artificial granite joint with hammered surfaces, an artificial regularly undulated joint, and a natural schist joint under different normal stress levels. These researchers presented the non-linear correlation of asperity degradation and normal stress by quantifying the amount of surface damage and considering the friction angle $\phi$ as a function of the normal stress $\sigma_n$, i.e., $\phi = f(\sigma_n)$. Correspondingly, Tang et al. (2016) suggested that the friction angle $\phi$ was a function of $\sigma_n$ and the tensile strength $\sigma_t$ of rock, i.e., $\phi = f(\sigma_n, \sigma_t)$ to represent nonlinearity. Figure 1 shows the nonlinearity of the set of experimental data. Therefore, nonlinearity is beyond the expression of the bilinear shear strength criterion (Patton 1966). Figure 2 shows an ideal nonlinear failure envelope of sheared joints. And as shown

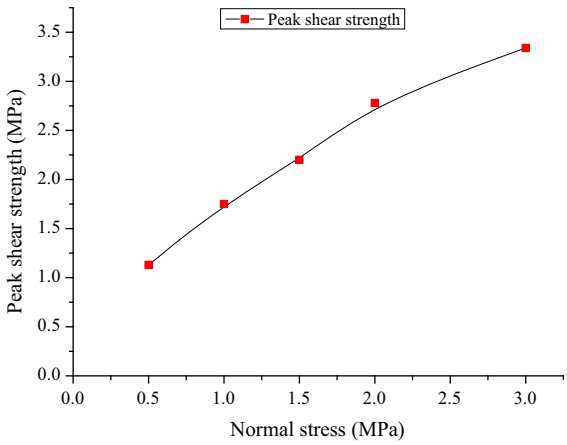


**Fig. 1** Set of experimental data from the direct shear test and its nonlinearity (data from Tang and Wong 2016)

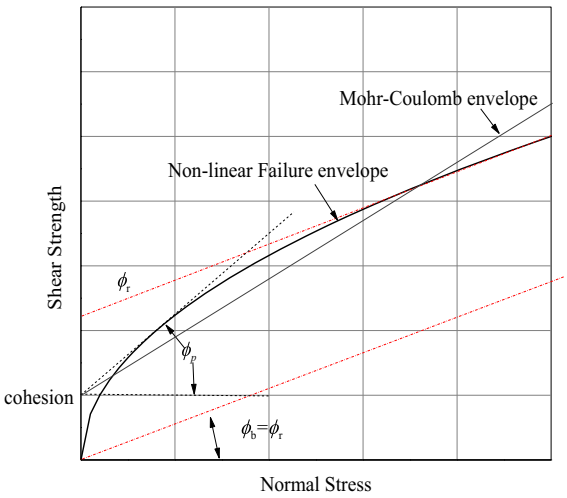


**Fig. 2** Non-linear failure envelope of sheared joints

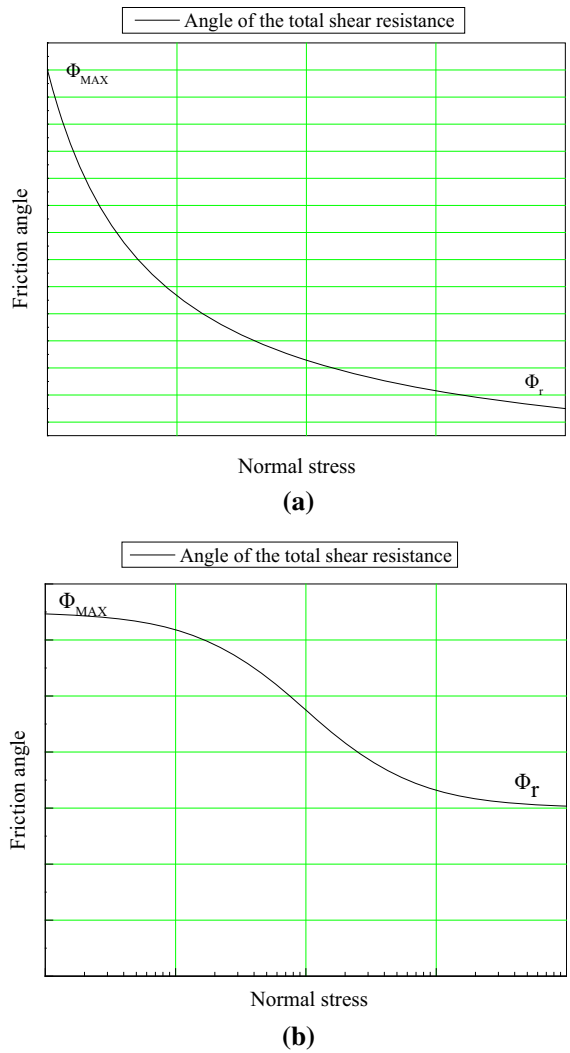


**Fig. 3** Non-linear variation of friction angle for the failure envelope. **a** rectangular coordinate plot. **b** Semi-log plot. (Reproduced with permission from Maksimović 1996)

in Fig. 2, if the traditional Mohr–Coulomb expression is used to present the failure envelope, then the friction angle is the inclination of the tangent line to the failure envelope, where it is a constant. But the non-linear variation of the friction angle for the failure envelope shown in Fig. 3a decreases with increasing normal stress level, and an "S" shape appears in the semi-log plot (as shown in Fig. 3b), as Homand et al. (2001) proposed, the Mohr–Coulomb criterion is not suitable for representing non-linearity of failure envelope.

As Barton (1973) described, the friction angle $\phi_P$ of the peak shear strength assumes the following form:

$$\phi_p = \phi_b + d_n + s_n, \tag{1}$$

where $\phi_b$ is the basic angle of friction, $d_n$ is the peak dilation angle, and $s_n$ is the contribution of asperities degradation.

The peak friction angle based on Coulomb's expression is expressed as the ratio of peak shear stress to normal stress (as shown in Fig. 4):

$$\frac{\tau_p}{\sigma_n} = \tan \phi_p. \tag{2}$$

Subsequently, Barton and Choubey (1977) proposed an empirical law (the JRC–JCS model) of friction for rock joints based on an extensive

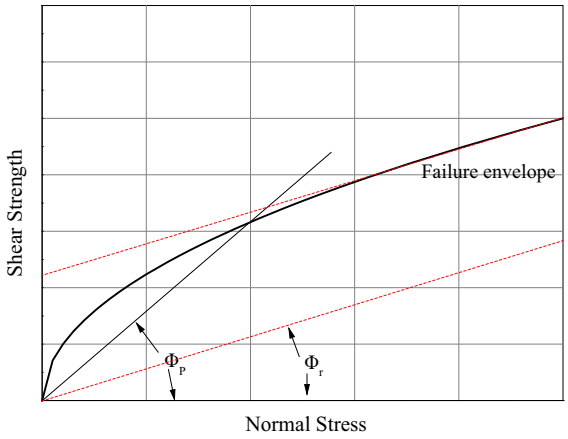


**Fig. 4** Friction angle diagram for the JRC–JCS model

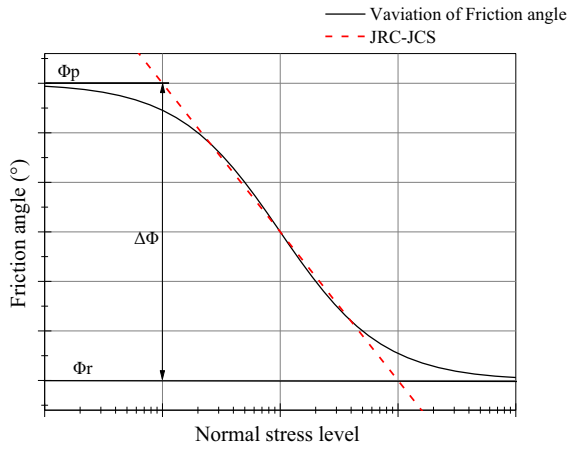


**Fig. 5** Friction angle comparison for the JRC–JCS model and the failure envelope in a semi-log plot

experiment on natural rock joints. The friction angle and shear strength, respectively, take the following forms:

$$\phi = \phi_r + \mathrm{JRC}\log\left(\frac{\mathrm{JCS}}{\sigma_n}\right), \tag{3}$$

and

$$\tau = \sigma_n \tan\left[\phi_r + \mathrm{JRC}\log\left(\frac{\mathrm{JCS}}{\sigma_n}\right)\right], \tag{4}$$

where $\phi_r$ is the residual friction angle, JRC is the joint roughness coefficient, and JCS is the joint compressive strength. For unweathered rock joints, the residual friction angle $\phi_r$ is equal to the basic friction angle ($\phi_b$), and JCS is equal to the uniaxial compressive of intact rock ($\sigma_c$). Therefore, it assumes peak friction angle is the inclination angle ($\phi$) of the line connecting the point on the failure envelope and the origin.

The comparison of friction variation in Fig. 5 shows a dotted line, which represents the variation of friction angle for the JRC–JCS model, and a continuous line, which denotes the variation of friction angle for the failure envelope. In the semi-log plot, the variation of the friction angle was represented by a negative linear correlation with normal stress in the JRC–JCS model (red dotted line shown in Fig. 5). Thus the best straight-line fit in the semi-log plot depends on the distribution of data points in the stress range from zero to a certain high stress level (Maksimović 1996). When the normal stress is in an appropriate range, the negative linear correlation is an excellent approximation for the variation of friction angle. However, the JRC–JCS model offers an overestimated or underestimated friction value when the normal stress offset is without this range (Maksimović 1992). Therefore, the JRC–JCS empirical criterion is a linear correlation that represents the non-linear variation of the friction angle in the moderately normal stress range in the semi-log plot. As a result, the friction value could be overestimated or underestimated in a lower or higher normal stress level range. So the JRC–JCS model's predicting results depend on the distribution of experimental data. In this case, when the experimental normal stress decreases to lower stress level, a good approximation could be supplied in the lower stress level, and a larger error could be produced for the higher stress level, and vice versa.

Maksimović (1992) proposed a hyperbolic relationship (as shown in Fig. 6) to describe the tangent angle ($\phi_T$) on the failure envelope in terms of the non-linearity of the failure envelope, which is written as follows:

$$\phi_T = \phi_b + \Delta\phi/(1 + \sigma_n/p_N), \tag{5}$$

where $\Delta\phi$ reflects the surface roughness of the discontinuity and the associated dilatancy effects at zero stress level and can be described as the "angle of maximum dilatancy," that occurs on an undamaged rugged surface, and $P_N$ is "the median angle pressure" and is equal to the value of the normal stress, where $\phi$=$\phi_b + \Delta\phi/2$ (Fig. 6). The strength and rigidity of the asperities that roughen the discontinuity surface are mainly reflected.

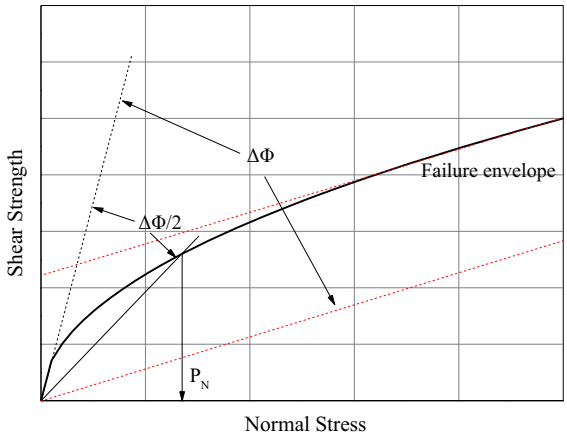


**Fig. 6** Definition of parameters for rock joint (from Maksimović 1996)

Shear strength can be expressed in terms of the tangent angle $\phi_T$ on the failure envelope and the apparent cohesion $c_T$, in Mohr–Coulomb form (Maksimović 1996):

$$\tau_p = c_T + \sigma_n \tan \phi_T. \quad (6)$$

The hyperbolic relationship proposed by Maksimović (1996) can better represent the non-linearity correlation of the friction angle and the normal stress than the JRC–JCS model for which a negative linear correlation was used to characterize the variation of friction angle. But it's hard to obtain the $P_N$ value. Figure 7 illustrates that the three lines that show the degradation of friction for $\Delta\phi$ equal to 30°, 20°, and 10° (note that $\phi_b$ is fixed to represents identical rock

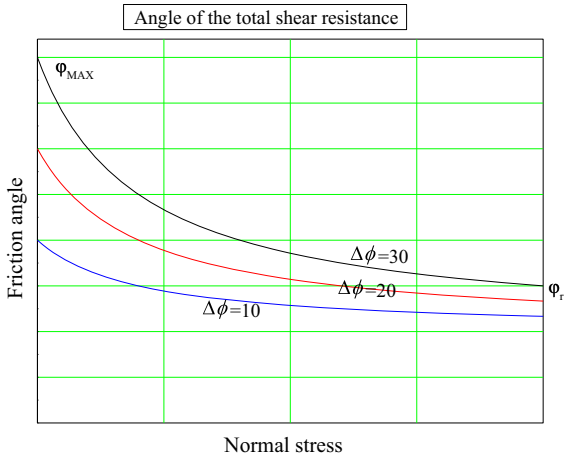


**Fig. 7** Degradation of friction angle by Maksimović (1996) ($\Delta\phi$ equal to 30°, 20°, and 10°)

joint types), in which each $\Delta\phi$ corresponding to certain surface roughness of the discontinuity. Thus, only one variation of friction path exists for certain surface roughness. Remarkably, the fixed friction degradation path requires further discussion on whether nonlinearity can be represented or not. In addition, the same degradation path should be considered uncertain for different surface morphologies. Thus, this model ignored the various degradation paths of friction and the influence of surface morphology. Apparent cohesion, which increases with normal stress, was introduced into Maksimović's model. If cohesion describes the physical and mechanical properties of the material, then it should be a constant. The principle that cohesion increases with increasing normal stress appears in the variation of friction under different normal stresses. Barton (2013, 2016) discussed this principle in his studies and proposed that Coulomb's expression is more appropriate for describing the non-linearity of the failure envelope.

Lee et al. (2001) observed that the degradation of the asperities of a rock joint under cyclic loading conditions followed exponential degradation laws, and a damage coefficient was introduced to connect the degradation of the joint asperity and the initial surface topography. Homand et al. (2001) proposed two shear strength criteria based on Eq. (1) by investigating the degradation of a joint asperity on three different rock joints. Each joint has a constant related to shear surface degradation and initial surface topography. Many studies (Grasselli and Egger 2003) have also shown that friction is correlated with the rock joint material, normal stress level, and surface morphology. Thereafter, researchers (Yang et al. 2016; Tang et al. 2016; Grasselli 2006; Zhang et al. 2016) established more complicated shear strength criteria by quantifying the surface morphology to overcome subjective determination of the joint roughness coefficient (JRC).

## 3 Modified Model and Discussion

The non-linearity of the rock joint failure envelope is associated with the joint material, normal stress level, and joint topography. The use of the traditional Mohr–Coulomb criterion to describe nonlinearity is inappropriate according to the aforementioned analysis. The inclination angle of the line that connects the point on

failure envelope and the origin could be used to express shear strength from frictional resistance. According to the friction component form for the peak shear strength (Eq. 3) (Barton 1973) and the hyperbolic type hypothesis (Maksimović 1996) for the tangent description on the failure envelope, which displays an S-shape in the semi-log plot, it assumes that the inclination angle of the line that connects the point on the failure envelope and origin (friction) obeys a hyperbolic law in a rectangular coordinate system (Fig. 3a) and shows an S-shape in the semi-log plot (Fig. 3b). Consequently, a modified hyperbolic type was adopted to describe the variation of the friction angle of failure envelope:

$$\phi = \phi_r + \Delta\phi/(1 + a\sigma_n/\mathrm{JCS}), \tag{7}$$

where $\phi_r$ is the residual friction angle (°), JCS is the joint compressive strength (MPa), $\sigma_n$ is the normal stress (MPa), $a$ is the coefficient related to the initial surface topography of joint and joint material properties and reflects the influence of initial surface topography and normal stress level on friction degradation for peak shear strength, $\Delta\phi$ is the difference between $\phi_{MAX}$ and $\phi_r$ (Fig. 3) (with a value determined by regression analysis), $\phi_{MAX}$ is the friction of the initial surface roughness of the discontinuity and the associated dilatancy effects at extremely low stress levels, and $\phi_r$ is the residual friction angle in accordance with Barton and Choubey (1977).

For Eqs. (7), $\sigma_n \to 0$, $\phi = \phi_r + \Delta\phi$, $\sigma_n \to +\infty$, $\phi = \Delta\phi_r$. Thus, Eqs. (1–8) show that the friction angle reaches a maximum for the maximum dilatancy at an extremely low stress, and it is an asymptote of the residual friction angle when the normal stress is relatively high (Fig. 3). The proposed model introduces coefficient $a$ to reflect the influence of the initial surface topography and the normal stress level on the friction degradation of the failure envelope. The coefficient was determined by regression analysis, and thus, it could better fit the degradation of friction (Fig. 8), and a more reliable result could be obtained. Coefficient $a$, which could assign an empirical value when no adequate experimental data are available, is also an option.

In the following sections, a statistical analysis and a comparison were conducted to verify the validity of the model.

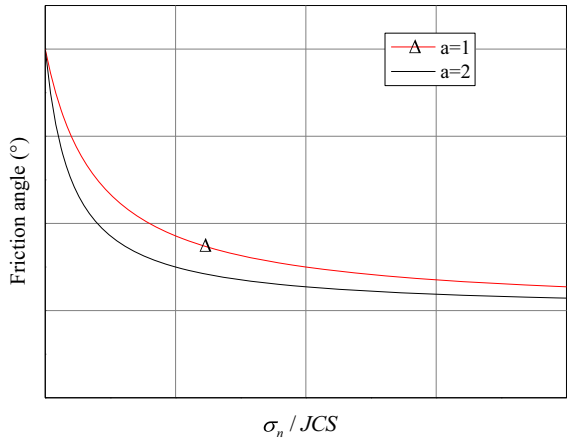


**Fig. 8** Degradation path of the friction angle in the proposed model

## 4 Verification

The results of the least-square regression analysis and the experimental data from (Tang and Wong 2016) were used to compare the existing criterion of the JRC–JCS model. The failure envelope can be obtained based on Eq. 7 with the following expression:

$$\tau = \sigma_n \tan(\phi_r + \Delta\phi/(1 + a\sigma_n/\mathrm{JCS})), \tag{8}$$

where $\phi_r$ is the residual friction angle (°), JCS is the joint compressive strength (MPa), $\sigma_n$ is the normal stress (MPa) and is an independent variable, $\tau$ is the peak shear strength (MPa) and is the dependent variable, and $\Delta\phi$ and a are undetermined coefficients.

The experimental data (Tang and Wong 2016),as show in Table 1, were collected from the direct shear test results performed on each group of samples with identical geometrical features under a constant normal load condition. Thus, the samples have similar surface morphologies (or joint roughness coefficients) for the same group. And joint compressive strength is the same because they were made up of the same material.

Table 1 shows comparison with experimental data of the direct shear test and calculated shear strength, and Table 2 presents the fitting parameters for joint groups J-I, J-II, and J-III. Figures 9a, 10b, and 11b illustrate the fitting results in the proposed model with a fitting coefficient greater than 0.95, and the residual (as shown in Figs. 9b, 10b and 11b) is randomly scattered on both sides of the horizontal axis. Thus, the proposed model is excellent in describing the nonlinearity of the failure envelope. Additionally, $\Delta\phi$

**Table 1** Comparison with experimental data of the direct shear test and calculated shear strength (experimental data from Tang and Wong 2016)

| Sample | Normal stress (MPa) | JCS (MPa) | JRC | $JRC_{cal}$ | $\tau/\sigma$ | Inclination (°) | Residual friction angle (°) | Peak shear strength (MPa) | Calculated peak shear strength | | | |
|---|---|---|---|---|---|---|---|---|---|---|---|---|
| | | | | | | | | | This paper (MPa) | | JRC–JCS (MPa) | |
| | | | | | | | | | Prediction | Error | Prediction | Error |
| Group J-I | 0.5 | 27.5 | 6.3 | 11.3 | 1.7 | 59.53 | 35 | 0.85 | 0.81 | − 0.04 | 0.71 | − 0.14 |
| Group J-I | 1 | 27.5 | 6.3 | 11.3 | 1.19 | 49.96 | 35 | 1.19 | 1.31 | 0.12 | 1.25 | 0.06 |
| Group J-I | 1.5 | 27.5 | 6.3 | 11.3 | 1.18 | 49.72 | 35 | 1.77 | 1.74 | − 0.03 | 1.38 | − 0.39 |
| Group J-I | 2 | 27.5 | 6.3 | 11.3 | 1.12 | 48.24 | 35 | 2.24 | 2.14 | − 0.1 | 2.21 | − 0.03 |
| Group J-I | 3 | 27.5 | 6.3 | 11.3 | 0.95 | 43.43 | 35 | 2.84 | 2.9 | 0.06 | 3.09 | 0.25 |
| Group J-II | 0.5 | 27.5 | 12.8 | 16.5 | 2.26 | 66.13 | 35 | 1.13 | 1.16 | 0.03 | 1.01 | − 0.12 |
| Group J-II | 1 | 27.5 | 12.8 | 16.5 | 1.75 | 60.26 | 35 | 1.75 | 1.75 | 0 | 1.65 | − 0.1 |
| Group J-II | 1.5 | 27.5 | 12.8 | 16.5 | 1.47 | 55.71 | 35 | 2.2 | 2.22 | 0.02 | 2.21 | 0.01 |
| Group J-II | 2 | 27.5 | 12.8 | 16.5 | 1.39 | 54.27 | 35 | 2.78 | 2.64 | − 0.14 | 2.73 | − 0.05 |
| Group J-II | 3 | 27.5 | 12.8 | 16.5 | 1.11 | 48.07 | 35 | 3.34 | 3.44 | 0.1 | 3.69 | 0.35 |
| Group J-III | 0.5 | 27.5 | 17.1 | 21.9 | 3.56 | 74.31 | 35 | 1.78 | 1.77 | − 0.01 | 1.65 | − 0.13 |
| Group J-III | 1 | 27.5 | 17.1 | 21.9 | 2.42 | 67.55 | 35 | 2.42 | 2.44 | 0.02 | 2.3 | − 0.12 |
| Group J-III | 1.5 | 27.5 | 17.1 | 21.9 | 1.93 | 62.57 | 35 | 2.89 | 2.95 | 0.06 | 2.9 | 0.01 |
| Group J-III | 2 | 27.5 | 17.1 | 21.9 | 1.76 | 60.33 | 35 | 3.51 | 3.41 | − 0.1 | 3.45 | − 0.06 |
| Group J-III | 3 | 27.5 | 17.1 | 21.9 | 1.4 | 54.46 | 35 | 4.2 | 4.23 | 0.03 | 4.46 | 0.26 |

**Table 2** Fitting parameters for joints

| Parameters | $\Delta\phi$ (°) | | $a$ | | Statistics | |
|---|---|---|---|---|---|---|
| | Value | Standard error value | Value | Standard error value | Reduced Chi-Sqr | Adj. R-square |
| Joint J-I | 33.94 | 7.76344 | 25.4499 | 9.94 | 0.0102 | 0.98 |
| Joint J-II | 42.45 | 3.72503 | 18.8500 | 3.33 | 0.0096 | 0.99 |
| Joint J-III | 48.89 | 1.20875 | 13.6014 | 0.86 | 0.0055 | 0.99 |

reflects the difference between the maximum friction angle of the initial surface roughness of the discontinuity and the associated dilatancy effects at extremely low stress levels and the residual friction angle at extremely high normal stress levels, which occur on completely damaged asperities. Hence, the friction angle of the peak shear strength increases with the JRC value under a low normal stress because of the sliding

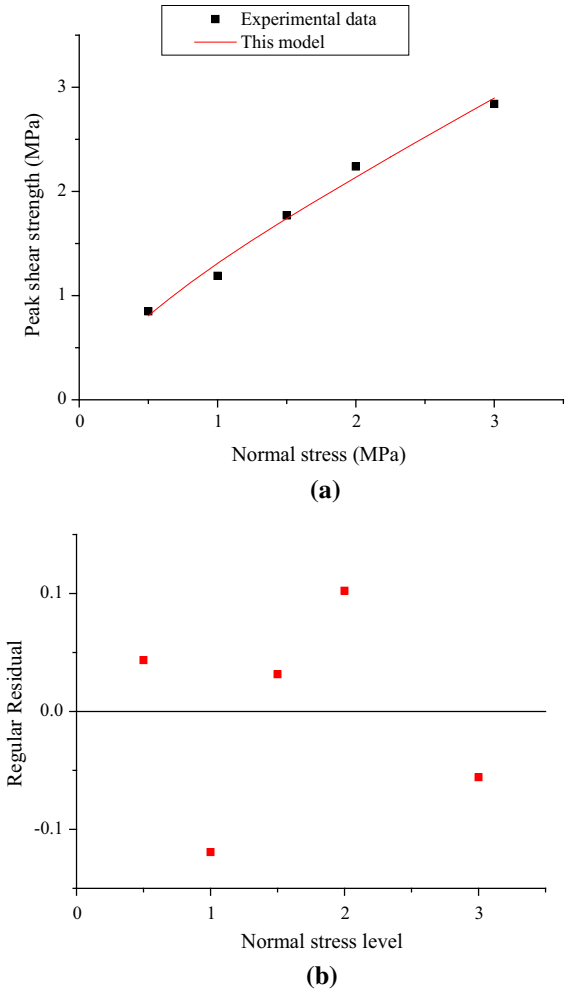


**Fig. 9** Analysis of the fitting result in joint group J-I

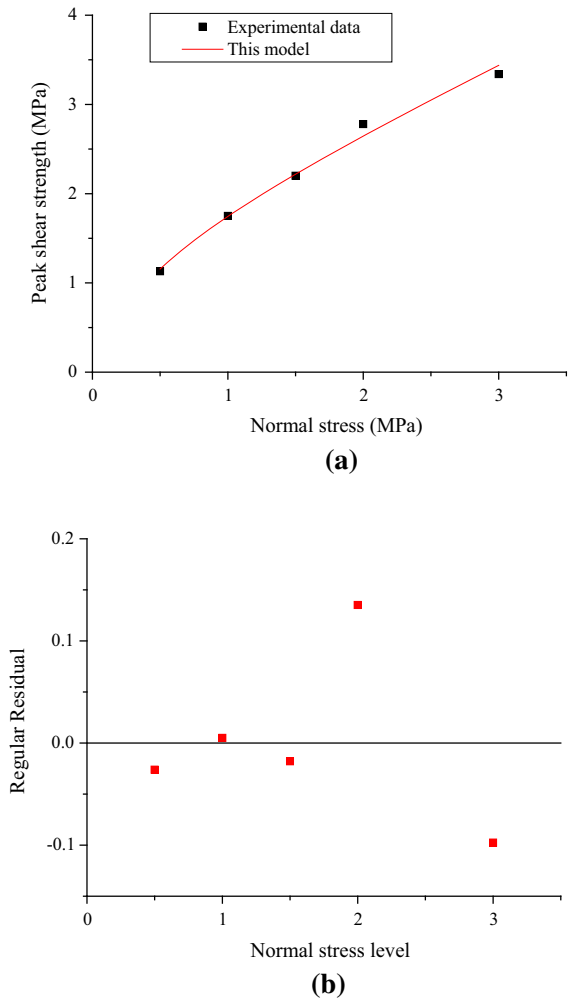


**Fig. 10** Analysis of the fitting result in joint group J-II

along the asperity. The residual friction angle is reached at an extremely high normal stress in which the asperities are completely damaged. Consequently, a large JRC implies an increase in the difference between the friction under low normal stress and that under high normal stress. Coefficient $\Delta\phi$ is equal to 33.94, 42.45, and 48.89 for joint groups J-I, J-II, and J-III, respectively, and the value increases as JRC increases based on the fitting results. Thus, $\Delta\phi$ satisfies the basic change rule. Coefficient $a$ is related to the initial surface joint topography and compressive strength, and it reflects the influence of the initial surface topography and the normal stress level on the friction degradation of the failure envelope. The effect of the shearing of asperities becomes more evident when the JRC is larger for the same normal stress level. Thus, the friction angle decreases rapidly with increasing normal stress level when the value of JRC increases, and thus $a$ appears to be larger. The performance of the $a$ value in the fitting results also satisfies the rule of basic change.

## 5 Comparison with the Existing JRC–JCS Criterion

The results are compared with the analysis results of the JRC–JCS model. The measured peak shear strength is relatively higher than the calculated values obtained using Barton's criterion when the JRC values are determined by the visual method. Hence, the value of JRC ($JRC_{cal}$) obtained by back-calculated of the

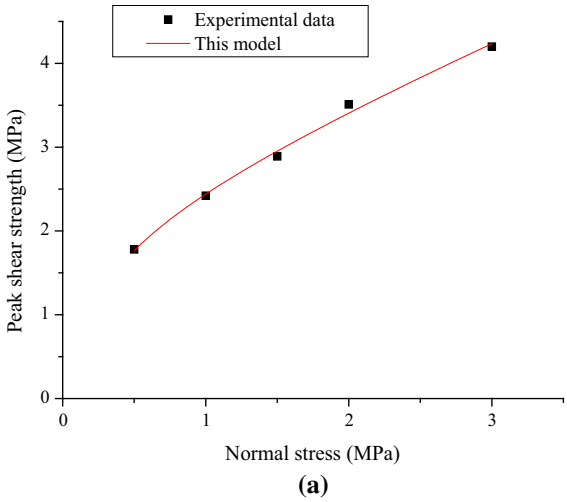


**Fig. 11** Analysis of the fitting result in joint group J-III

direct shear test results is input into the JRC–JCS model (Xia et al. 2014). Table 1 shows the comparison of the experimental data with the calculated shear strength from the proposed and JRC–JCS models. Certain deviations can be observed between the experimental data and the predicted values, which contain model and measurement errors. As mentioned in Sect. 2, JRC–JCS model's predicting results depend on the distribution of experimental data. Correspondingly, the shear strength predicted by the JRC–JCS model tends to be larger than the experimental data when the normal stress is relatively high (Table 1). Figures 12, 13, and 14 show the comparisons of the failure envelope calculated by the proposed and JRC–JCS models for joint groups J-I, J-II, and J-III, respectively. These figures illustrate that the failure

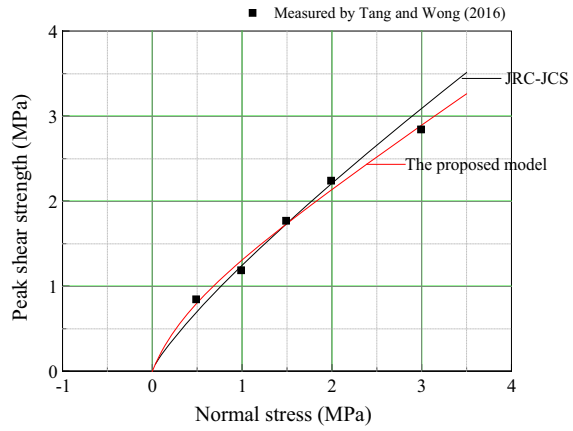


**Fig. 12** Comparison of the failure envelope calculated by the proposed and JRC–JCS models for joint group J-I

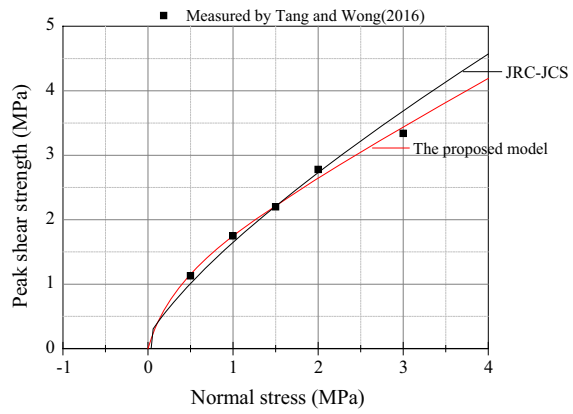


**Fig. 13** Comparison of the failure envelope calculated by the proposed and JRC–JCS models for joint group J-II

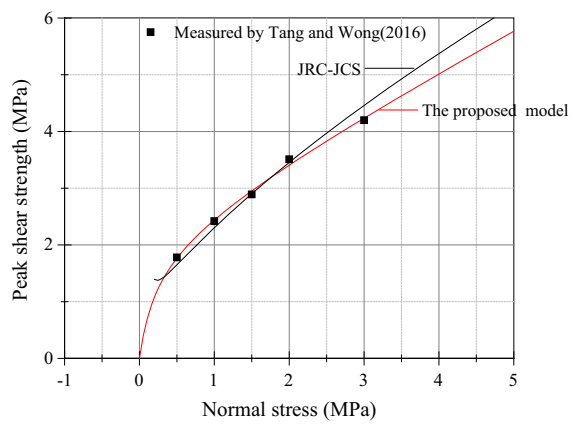


**Fig. 14** Comparison of the failure envelope calculated by the proposed and JRC–JCS models for joint group J-III

envelope of JRC–JCS is offset upward for high normal stress. Thus, deviation increases with increasing normal stress. In the semi-log plot, a negative linear correlation with normal stress was used to represent the variation of friction in the JRC–JCS model (as shown in Fig. 5). As a result, the non-linearity of the failure envelope cannot be expressed satisfactorily. The slope of the line changes with the distribution of the data points. Consequently, an overestimated or underestimated friction value can result for lower or higher normal stress levels.

No significant deviation is observed between the predicted value of the proposed model and the experimental data at relatively high normal stress. Furthermore, when the joint roughness coefficient significantly changes, the predicted value does not deviate from its experimental data at lower and higher normal stresses. Therefore, the proposed model adapts well to the variation trend of the friction angle and produces an accurate predicted value. When the experimental data are taken from a small range of normal stress, the model proposed in this study fails to supply the offset predicted shear strength value for the other normal stress sections, and it will be helpful for predicting shear strength at full normal stress level. Coefficients $\Delta\phi$ and $a$ are determined by regression analysis. Thus, the proposed model avoids direct connection with surface morphology, which is convenient for practical use.

## 6 Conclusions

The non-linearity of the failure envelope for rock joint shearing and the corresponding variation of friction were studied. A modified hyperbolic function, $\tau = \sigma_n \tan(\phi_r + \Delta\phi/(1 + a\sigma_n/\mathrm{JCS}))$, was adopted to describe the degradation of the peak friction angle. The coefficient $a$ is related to the initial surface topography of the joint and joint compressive strength, and it reflects the influence of the initial surface topography and normal stress level on the friction degradation of the failure envelope. Additionally, $\Delta\phi$ reflects the difference between the maximum friction angle $\phi_{MAX}$ of the initial surface roughness of the discontinuity and the associated dilatancy effects at extremely low stress levels and the residual friction angle $\phi_r$. In this model, $\sigma_n \to 0$, $\phi = \phi_r + \Delta\phi$; $\sigma_n \to +\infty$, $\phi = \phi_r$, and thus, the friction angle reaches a maximum for the maximum dilatancy at extremely low stress and is an asymptote of the ultimate friction when the normal stress is relatively high. The proposed model meets the variation of friction path well, owing to the introduction of $a$. Thus, it could better fit the degradation of friction, and a reliable result can be obtained. Furthermore, coefficient $a$ could assign an empirical value when no experimental data are available.

A statistical analysis of the experimental data verified the validity of the proposed model, which offered an excellent method for characterizing the non-linearity of the failure envelope. In addition, $\Delta\phi$ and $a$ satisfy the basic change rule according to the definition. The proposed model offered higher accuracy predictions than the JRC–JCS criterion, especially at high normal stress levels. Moreover, the proposed model overcomes the overestimation or underestimation at lower or larger normal stress levels of the JRC–JCS empirical model. It will be helpful for predicting shear strength at full normal stress level.

**Acknowledgements** This paper gets its funding from project (51474249, 51774322, 41562016) supported by National Natural Science Foundation of China; Project (2016CX019) supported by Innovation-driven Plan in Central South University; Project (2017zzts534) supported by the Fundamental Research Funds for the Central Universities of Central South University. The authors wish to acknowledge these supports.

## References

Asadollahi P, Tonon F (2010) Constitutive model for rock fractures: revisiting Barton's empirical model. Eng Geol 113:11–32

Bahaaddini M, Sharrock G, Hebblewhite BK (2013) Numerical direct shear tests to model the shear behaviour of rock joints. Comput Geotech 51:101–115

Bandis S, Lumsden A, Barton N (1983) Fundamentals of rock joint deformation. Int J Rock Mech Min Sci Geomech Abstr 20:249–268

Barton N (1973) Review of a new shear-strength criterion for rock joints. Eng Geol 7:287–332

Barton N (2013) Shear strength criteria for rock, rock joints, rockfill and rock masses: problems and some solutions. J Rock Mech Geotech Eng 5:249–261

Barton N (2016) Non-linear shear strength for rock, rock joints, rockfill and interfaces. Innov Infrastruct Solut 1:30

Barton N, Choubey V (1977) The shear strength of rock joints in theory and practice. Rock Mech 10:1–54

Grasselli G (2006) Manuel Rocha medal recipient shear strength of rock joints based on quantified surface description. Rock Mech Rock Eng 39:295

Grasselli G, Egger P (2003) Constitutive law for the shear strength of rock joints based on three-dimensional surface parameters. Int J Rock Mech Min Sci 40:25–40

Homand F, Belem T, Souley M (2001) Friction and degradation of rock joint surfaces under shear loads. Int J Numer Anal Meth Geomech 25:973–999

Lee H, Park Y, Cho T, You K (2001) Influence of asperity degradation on the mechanical behavior of rough rock joints under cyclic shear loading. Int J Rock Mech Min Sci 38:967–980

Maksimović M (1992) New description of the shear strength for rock joints. Rock Mech Rock Eng 25:275–284

Maksimović M (1996) The shear strength components of a rough rock joint. Int J Rock Mech Min Sci Geomech Abstr 33:769–783

Misra A (2002) Effect of asperity damage on shear behavior of single fracture. Eng Fract Mech 69:1997–2014

Patton FD (1966) Multiple modes of shear failure in rock. In: Proc. 1st international congress on rock mechanics, Lisbon, pp 509–513

Serrano A, Olalla C, Galindo RA (2014) Micromechanical basis for shear strength of rock discontinuities. Int J Rock Mech Min Sci 70:33–46

Tang ZC, Wong LNY (2016) New criterion for evaluating the peak shear strength of rock joints under different contact states. Rock Mech Rock Eng 49:1191–1199

Tang ZC, Jiao YY, Wong LNY, Wang XC (2016) Choosing appropriate parameters for developing empirical shear strength criterion of rock joint: review and new insights. Rock Mech Rock Eng 49:1–12

Wan W, Liu J, Liu J (2018) Effects of asperity angle and infill thickness on shear characteristics under constant normal load conditions. Geotech Geol Eng 1–7. https://doi.org/10.1007/s10706-018-0447-5

Xia CC, Tang ZC, Xiao WM, Song YL (2014) New peak shear strength criterion of rock joints based on quantified surface description. Rock Mech Rock Eng 47:387–400

Yang J, Rong G, Hou D, Peng J, Zhou C (2016) Experimental study on peak shear strength criterion for rock joints. Rock Mech Rock Eng 49:821–835

Zhang X, Jiang Q, Chen N, Wei W, Feng X (2016) Laboratory investigation on shear behavior of rock joints and a new peak shear strength criterion. Rock Mech Rock Eng 49:3495–3512

Zhao J (1997) Joint surface matching and shear strength part B: JRC–JMC shear strength criterion. Int J Rock Mech Min Sci 34:179–185